Supplementary Information

for the article

'Adsorption of wastewater pollutants on amorphous TiO_2: an atomistic simulation study'

DOI: 10.1039/d5ma01085c
in: Materials Advances by the Royal Society of Chemistry
2026

Maria von Einem[a,*], Filippo Balzaretti[a,b], Manuela Romero[a], Wilke Dononelli[a,c,d], Lucio Colombi Ciacchi[a,c], Giancarlo Franzese[e] and Susan Köppen-Hannemann[a,c,‡]

[a] *Hybrid Materials Interfaces Group, Faculty of Production Engineering and Bremen Center for Computational Materials Science, University of Bremen, Bremen 28359, Germany.*
[b] *Chemistry & Biochemistry Department, University of California, Santa Cruz, California 95064, United States.*
[c] *MAPEX Center for Materials and Processes, University of Bremen, Bremen 28359, Germany.*
[d] *Institute for Physical and Theoretical Chemistry, University of Bremen, Bremen 28359, Germany.*
[e] *Secció de Física Estadística i Interdisciplinària -Departament de Física de la Matèria Condensada, Universitat de Barcelona, Martí i Franquès 1, Barcelona, 08028, Spain & Institut de Nanociència i Nanotecnologia, Universitat de Barcelona, Martí i Franquès 1, Barcelona, 08028, Spain.*
[*] First author, e-mail: voneinem@uni-bremen.de
‡ Corresponding author, e-mail: koeppen@uni-bremen.de

Supplementary Information

A.1 Partial charges and functional groups

In the following the pollutants are shown with their structure, partial charges and functional groups (Fig. A.1.1 - A.1.7). The color code and abbreviation for the functional groups can be taken from Tab. A.1.1.

Table A.1.1 Legend of the functional groups, their abbreviations and color codes used in this work

functional group	abbreviation	structure and color
amino	-NH_2	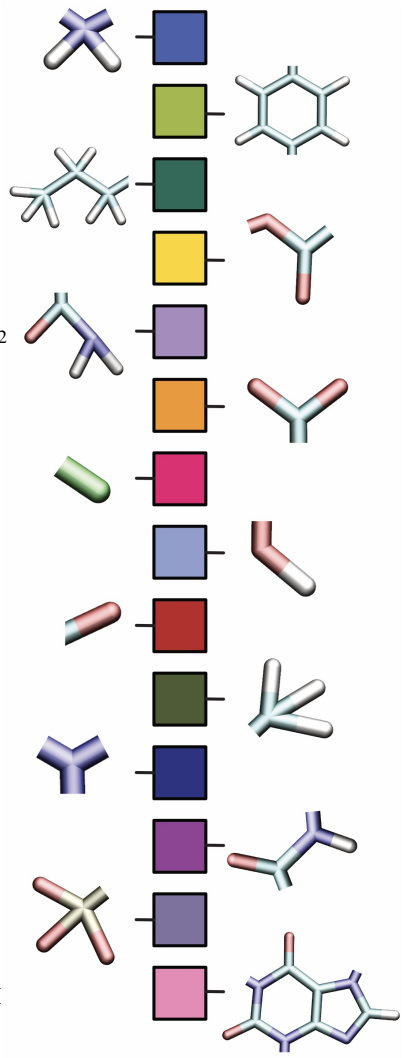
benzol	-C_6H_x	
hydrocarbon	-C_xH_x	
carbonylic acid	-OCO	
carboxamide	-$CONH_2$	
carboxylate	-COO^-	
chloride	-Cl	
hydroxyl	-OH	
keton	-CO	
methyl	-CH_3	
nitrogen	-N	
peptide	-CONH	
phosphonate	-PO_3^{2-}	
purin	-C_5N_4H	

A.2 Glyphosate and tetracycline structures

In literature different structures for GGG^{-2} and TTR^{-2} are reported.

The single deprotonated form of glyphosate (GGG^{-1}) is favored in zwitterionic form,[1–3] but for the double deprotonated form (GGG^{-2}) two structure suggestions exist: it is either bound to the nitrogen (zwitterionic form, Fig. A.2.1 A)[4–6] or to one oxygen of the phosphonate group (Fig. A.2.1 B)[1–3]. In Sprankle *et al.*[4] the zwitterionic form alongside pKa values are presented, found through titration curves and a dissociation order by the evaluation of similar compounds. More recent studies report the latter structure for GGG^{-2}, based on DFT calculations[1,3] as well as potentiometry, calorimetry and NMR spectroscopy[2]. Peixoto *et al.*[1] report only small differences in relative electrostatic free energy for both forms in PCM water for GGG^{-2} in certain configurations. Sadatsharifi *et al.*[3] show that a structure for GGG^{-2} in implicit SMD water with an intramolecular H-bond between the carboxylate and phosphonate group, that is positioning the hydrogen just across the nitrogen, is the energetically most stable configuration. Hence, they conclude that this configuration could be the reason for contradictory results from the past.

Given the state of the art, we considered using the non-zwitterionic form of glyphosate, but the force field did not provide any parameter for a phosphonate group with one bound hydrogen. Since the parametrization of the TiO_2 surface was done with AMBER99SB, we were not able to switch force fields and a complete reparametrization of glyphosate was beyond the scope of this study. Therefore we decided to use the zwitterionic form of glyphosate.

For TTR two chronological deprotonation orders are discussed for increasing pH values. Zuo *et al.*[7] report a hydrolysis of sites (3, 4, 12, 10) O7, N1, O2, O (site nomenclature corresponding to figure A.1.5 and A.1.6), while Amat *et al.*[8] suggest orders with a switched second and third deprotonation (3, 12, 4, 10 - O7, O2, N1, O). Amat *et al.*[8] used the Time Dependent Density Functional Theory (TD-DFT) method and compared the results to experimental absorption spectra with fairly good agreement. For the second deprotonation no significant difference in the computed spectra could be found between [3, 4] and [3, 12], but the pKa of [3, 12] is lower. Therefore they conclude that the order should be 3, 12, 4, 10. Zuo *et al.*[7] also performed calculations and experiments with an order 3, 4, 12, 10 as a result.
We calculated geometry optimizations and CHELPG charges for both TTR^{-1} structures ([3, 4] and [3, 12]) in vacuum. The [3, 12] structure could not be stabilized without implicit water and an additional bias without showing proton jumps. Since it was more stable even in vacuum, we decided to take the [3, 4] TTR^{-1} conformation.

A.3 TiO_2 model

The TiO_2 model used here was developed by some authors of this manuscript and is first published in Derr *et al.*[9]. To get a better overview of this model snapshots of the surface (Fig. A.3.1) as well as the charges and numbers of surface sites (Tab. A.3.1) are shown here.

ACE^{0}

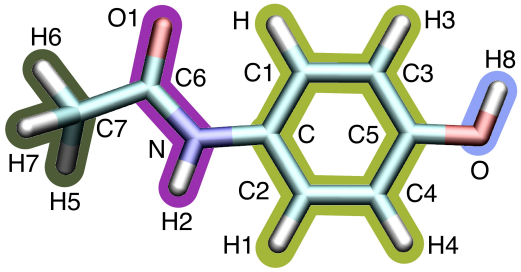

ASA^{-1}

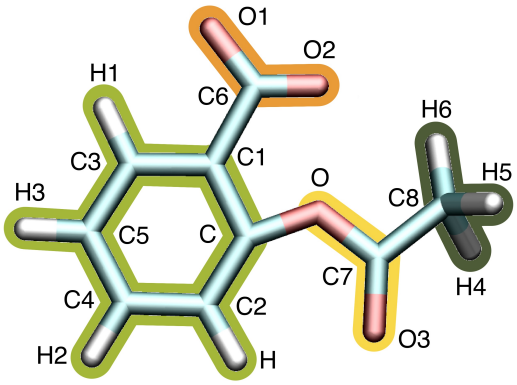

atom	charge (e)	atom	charge (e)
O	-0.564751	C7	-0.563745
O1	-0.582179	H	0.191397
N	-0.682995	H1	0.191397
C	0.440752	H2	0.340642
C1	-0.302969	H3	0.168256
C2	-0.302969	H4	0.168256
C3	-0.269162	H5	0.149801
C4	-0.269162	H6	0.149801
C5	0.380122	H7	0.149801
C6	0.802994	H8	0.404713

atom	charge (e)	atom	charge (e)
O	-0.458665	C6	0.667202
O1	-0.694722	C7	0.856868
O2	-0.694722	C8	-0.591579
O3	-0.577699	H	0.132968
C	0.334873	H1	0.141993
C1	0.008595	H2	0.105755
C2	-0.275735	H3	0.107216
C3	-0.190534	H4	0.152022
C4	-0.143573	H5	0.152022
C5	-0.184307	H6	0.152022

Fig. A.1.1 Partial charges, atom names and assigned functional groups of ACE^{0} and ASA^{-1}. The functional groups are methyl (dark olive), peptide (violet), benzol (light green), hydroxyl (light blue), carboxylate (orange) and carbonylic acid (yellow).

BEN^0

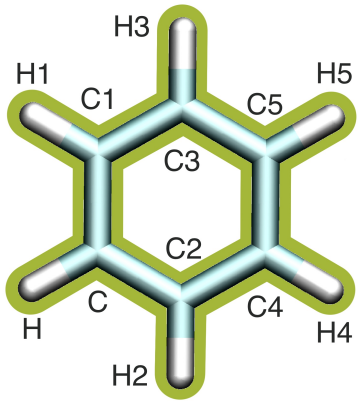

atom	charge (e)	atom	charge (e)
C	-0.114326	H	0.114326
C1	-0.114326	H1	0.114326
C2	-0.114326	H2	0.114326
C3	-0.114326	H3	0.114326
C4	-0.114326	H4	0.114326
C5	-0.114326	H5	0.114326

DCL^0

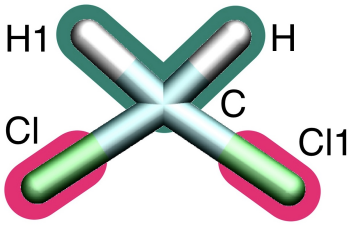

atom	charge (e)	atom	charge (e)
Cl	-0.076664	H	0.197525
Cl1	-0.076664	H1	0.197525
C	-0.241722		

CAF^0

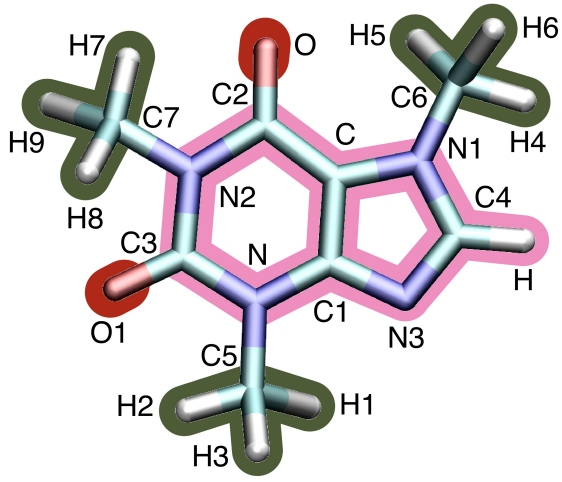

atom	charge (e)	atom	charge (e)
O	-0.523693	C6	-0.562653
O1	-0.514144	C7	-0.305235
N	-0.120396	H	0.147913
N1	0.360635	H1	0.144968
N2	-0.224838	H2	0.144968
N3	-0.522907	H3	0.144968
C	-0.542529	H4	0.192099
C1	0.486642	H5	0.192099
C2	0.658954	H6	0.192099
C3	0.551605	H7	0.136594
C4	0.033313	H8	0.136594
C5	-0.34365	H9	0.136594

Fig. A.1.2 Partial charges, atom names and assigned functional groups of BEN^0, DCL^0 and CAF^0. The functional groups are benzol (light green), methyl (dark olive), ketone (dark red), purine (light pink), hydrocarbon (dark green) and chloride (pink).

CBZ^{0}

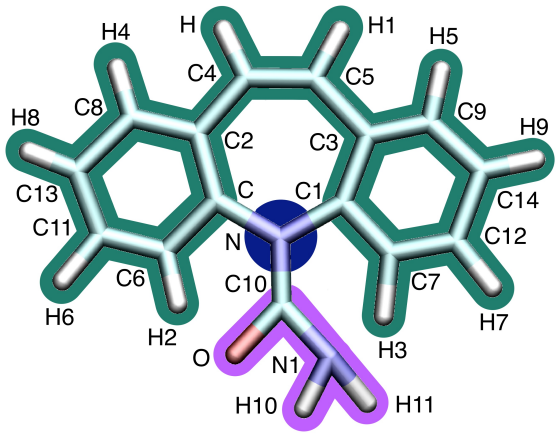

atom	charge (e)	atom	charge (e)
O	-0.554671	C12	-0.140178
N	-0.306995	C13	-0.11638
N1	-0.834106	C14	-0.11638
C	0.163602	H	0.146051
C1	0.163602	H1	0.146051
C2	0.194498	H2	0.157767
C3	0.194498	H3	0.157767
C4	-0.245816	H4	0.141396
C5	-0.245816	H5	0.141396
C6	-0.19421	H6	0.132687
C7	-0.19421	H7	0.132687
C8	-0.231699	H8	0.129057
C9	-0.231699	H9	0.129057
C10	0.704288	H10	0.358967
C11	-0.140178	H11	0.358967

GGG^{-2}

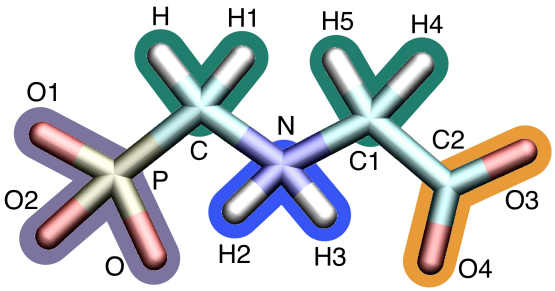

atom	charge (e)	atom	charge (e)
P	1.160762	C1	-0.289496
O	-0.95387	C2	0.841099
O1	-0.95387	H	0.118282
O2	-0.95387	H1	0.118282
O3	-0.82576	H2	0.199256
O4	-0.82576	H3	0.199256
N	0.287488	H4	0.11695
C	-0.355699	H5	0.11695

Fig. A.1.3 Partial charges, atom names and assigned functional groups of CBZ^{0} and GGG^{-2}. The functional groups are hydrocarbon (dark green), nitrogen (dark blue), carboxamide (light violet), phosphonate (dark violet), amino (blue) and carboxylate (orange).

IBU^{-1}

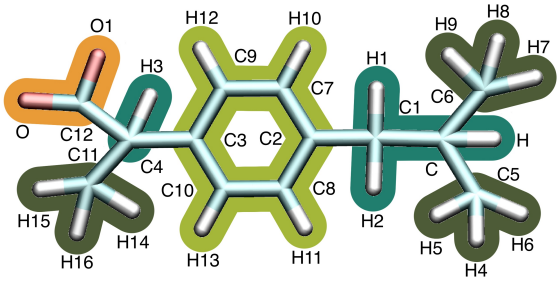

SLC^{-1}

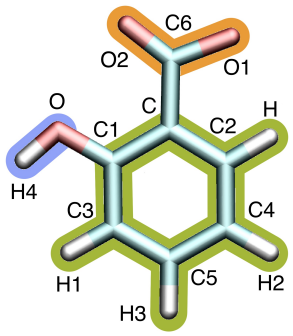

atom	charge (e)	atom	charge (e)
O	-0.741524	H1	0.078588
O1	-0.741524	H2	0.078588
C	0.739627	H3	-0.052256
C1	-0.499409	H4	0.115637
C2	0.379029	H5	0.115637
C3	0.082211	H6	0.115637
C4	0.204929	H7	0.115637
C5	-0.566831	H8	0.115637
C6	-0.566831	H9	0.115637
C7	-0.349719	H10	0.143261
C8	-0.349719	H11	0.143261
C9	-0.165344	H12	0.12926
C10	-0.165344	H13	0.12926
C11	-0.365001	H14	0.061698
C12	0.700049	H15	0.061698
H	-0.123477	H16	0.061698

atom	charge (e)	atom	charge (e)
O	-0.509959	C5	-0.131568
O1	-0.729267	C6	0.730151
O2	-0.729267	H	0.130591
C	-0.021455	H1	0.116089
C1	0.303807	H2	0.10324
C2	-0.1741	H3	0.100532
C3	-0.33555	H4	0.355412
C4	-0.208656		

Fig. A.1.4 Partial charges, atom names and assigned functional groups of IBU^{-1} and SLC^{-1}. The functional groups are carboxylate (orange), benzol (light green), hydrocarbon (dark green), methyl (dark olive), hydroxyl (light blue).

TTR^{-1}

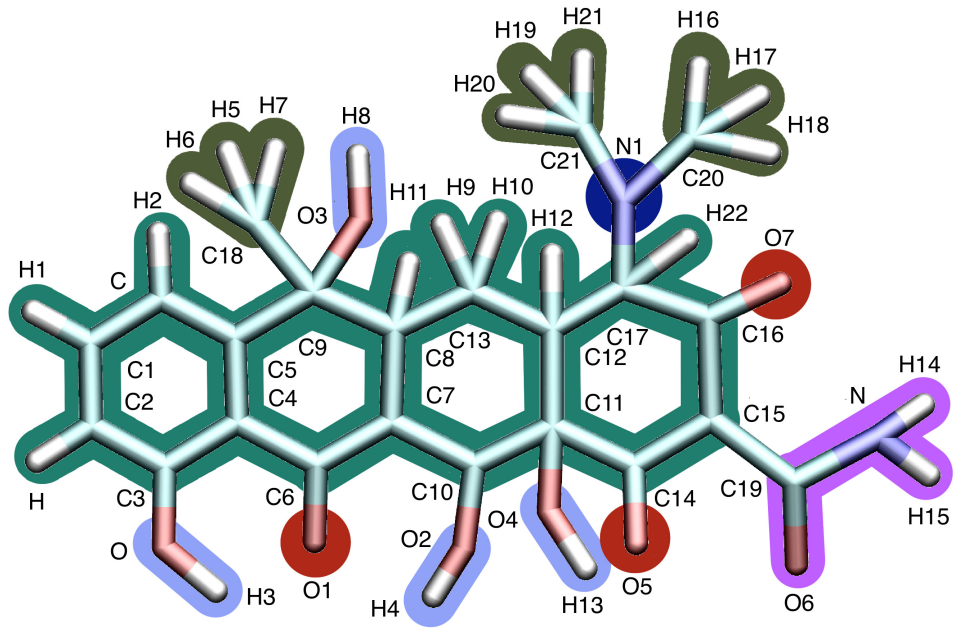

atom	charge (e)	atom	charge (e)	atom	charge (e)	atom	charge (e)
C	-0.319013	C14	0.471382	H5	0.107614	H14	0.347874
C1	-0.076816	C15	-0.535467	H6	0.107614	H15	0.347874
C2	-0.34442	C16	0.480735	H7	0.107614	O7	-0.616111
C3	0.547911	C17	-0.328372	H8	0.389076	N1	-0.05522
C4	-0.454739	H	0.169332	H9	0.121383	C20	-0.365374
C5	0.17145	H1	0.120532	H10	0.121383	C21	-0.365374
C6	0.710283	H2	0.147053	H11	0.009704	H16	0.114312
C7	-0.742365	O	-0.615964	H12	-0.01682	H17	0.114312
C8	0.567974	H3	0.447844	O4	-0.614769	H18	0.114312
C9	0.315109	O1	-0.636137	H13	0.374489	H19	0.114312
C10	0.530214	O2	-0.467258	O5	-0.490764	H20	0.114312
C11	-0.077406	H4	0.415242	C19	0.724951	H21	0.114312
C12	0.63768	O3	-0.654455	O6	-0.596311	H22	0.137281
C13	-0.654165	C18	-0.45754	N	-0.83061		

Fig. A.1.5 Partial charges, atom names and assigned functional groups of TTR^{-1}. The functional groups are hydrocarbon (dark green), methyl (dark olive), hydroxyl (light blue), ketone (dark red) and carboxamide (light violet).

TTR^{-2}

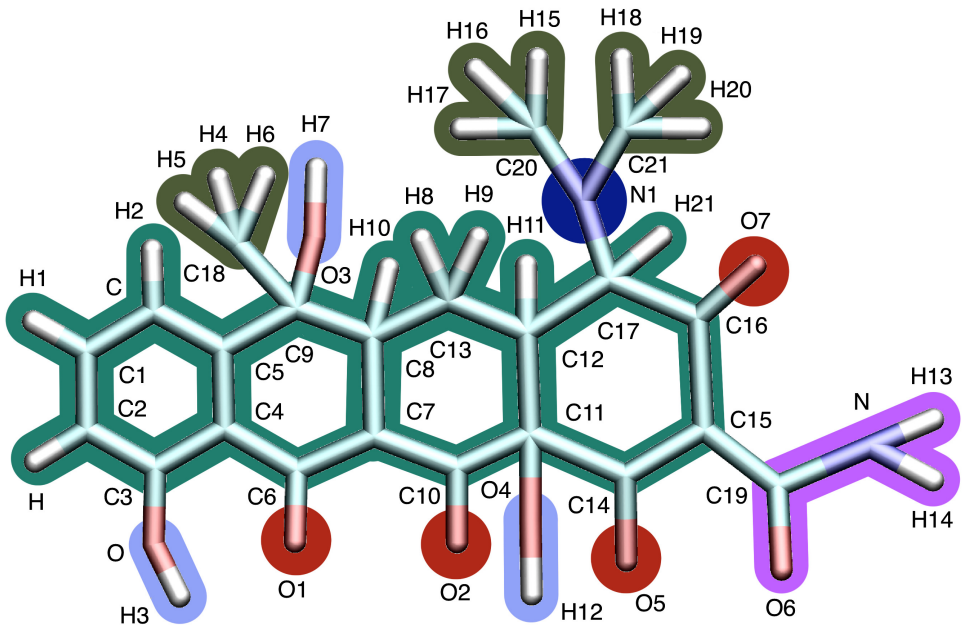

atom	charge (e)	atom	charge (e)	atom	charge (e)	atom	charge (e)
C	-0.403129	C14	0.757626	H5	0.138157	H14	0.411595
C1	-0.036109	C15	-0.686054	H6	0.138157	O7	-0.733254
C2	-0.429653	C16	0.671033	H7	0.439776	N1	-0.079604
C3	0.608088	C17	-0.581593	H8	0.176252	C20	-0.393699
C4	-0.548648	H	0.200273	H9	0.176252	C21	-0.393699
C5	0.227931	H1	0.143467	H10	-0.018864	H15	0.134158
C6	0.701335	H2	0.178317	H11	-0.13924	H16	0.134158
C7	-0.721372	O	-0.703353	O4	-0.634297	H17	0.134158
C8	0.468953	H3	0.474379	H12	0.385407	H18	0.134158
C9	0.500168	O1	-0.726212	O5	-0.694294	H19	0.134158
C10	0.569182	O2	-0.6557	C19	0.806254	H20	0.134158
C11	-0.313078	O3	-0.775989	O6	-0.728471	H21	0.18226
C12	1.180531	C18	-0.555921	N	-0.930621		
C13	-1.007239	H4	0.138157	H13	0.411595		

Fig. A.1.6 Partial charges, atom names and assigned functional groups of TTR^{-2}. The functional groups are hydrocarbon (dark green), methyl (dark olive), hydroxyl (light blue), ketone (dark red) and carboxamide (light violet).

VLP^{-1}

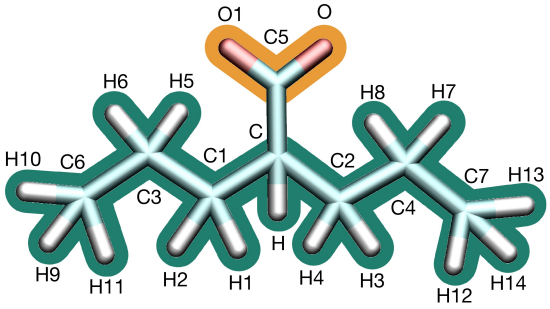

atom	charge (e)	atom	charge (e)
O	-0.751574	H3	-0.023266
O1	-0.751574	H4	-0.023266
C	-0.057511	H5	-0.042251
C1	-0.016994	H6	-0.042251
C2	-0.016994	H7	-0.042251
C3	0.298847	H8	-0.042251
C4	0.298847	H9	0.065994
C5	0.712770	H10	0.065994
C6	-0.408183	H11	0.065994
C7	-0.408183	H12	0.065994
H	-0.033347	H13	0.065994
H1	-0.023266	H14	0.065994
H2	-0.023266		

Fig. A.1.7 Partial charges, atom names and assigned functional groups of VLP^{-1}. The functional groups are carboxylate (orange) and hydrocarbon (dark green).

A

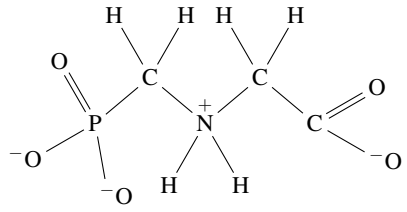

zwitterionic form

B

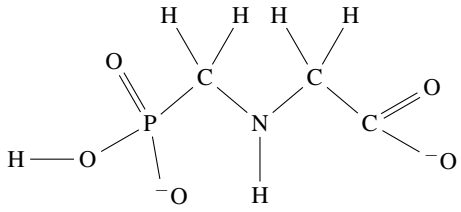

Fig. A.2.1 Glyphosate structures for the double deprotonated form that are reported in literature. A) shows the zwitterionic form, while B) depicts an alternative, non-zwitterionic version.

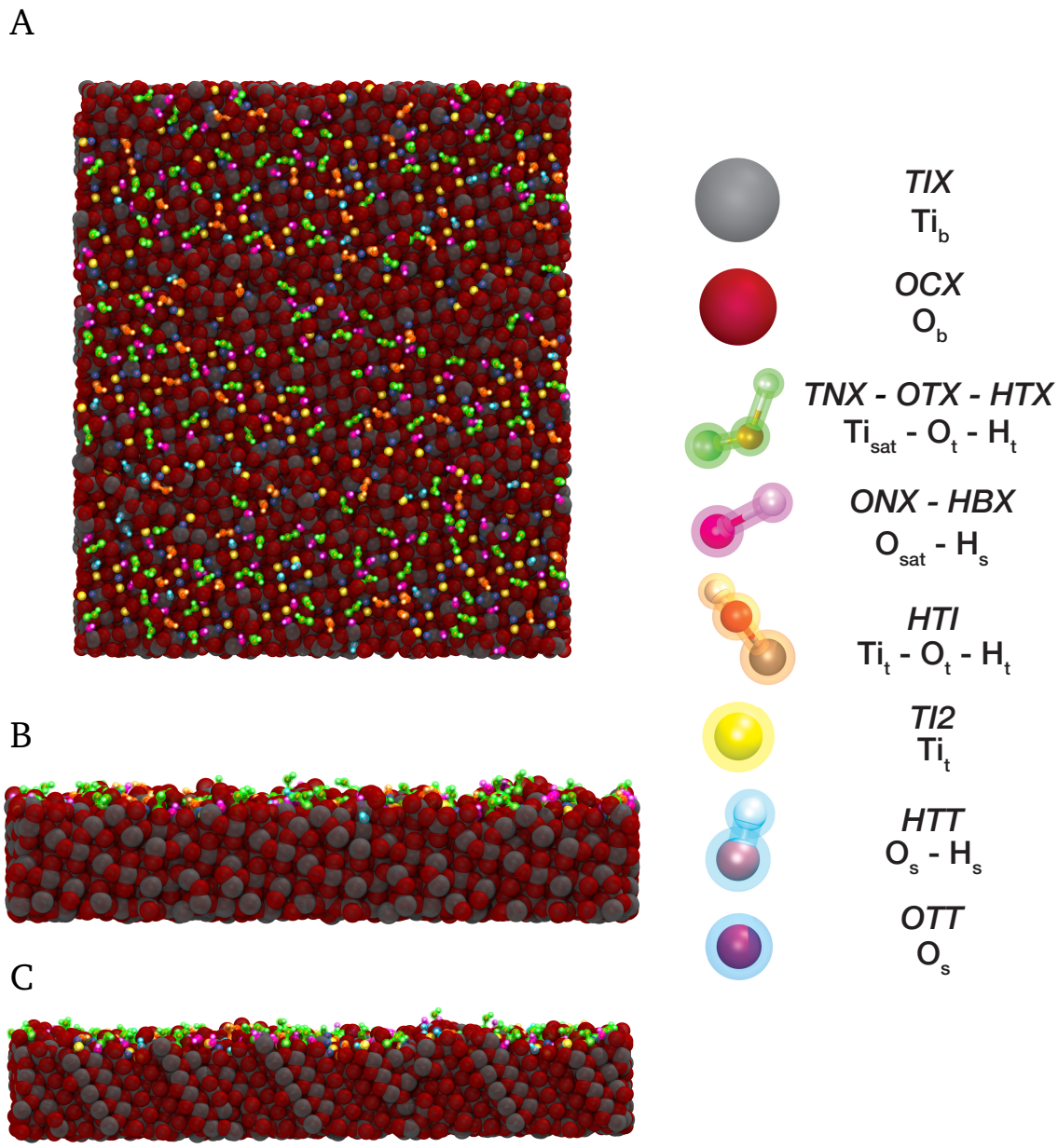

Fig. A.3.1 A) Top view and the two side views (B and C) of the amorphous TiO_2 surface slab model. Bulk titanium (Ti_b/*TIX*) and oxygen (O_b/*OCX*) atoms are shown as van der Waals spheres, the colored CPK atoms are the passive and active surface sites: Ti_{sat}-O_t-H_t - *TNX*/*OTX*/*HTX* (green), O_{sat}-H_s - *ONX*/*HBX* (pink), Ti_t-O_t-H_t - *HTI* (orange), Ti_t - *TI2* (yellow), O_s-H_s - *HTT* (light blue) and O_s - *OTT* (dark blue).

Table A.3.1 Quantity and partial charges of TiO_2 model atom types, including surface sites

atom	residue	quantity	charge (e)	note
Ti_b	*TIX*	6502	1.78	bulk titanium atom
O_b	*OCX*	13612	-0.891	bulk oxygen atom
Ti_{sat}	*TNX*	234	1.304 to 1.913	4-fold or less coordinated surface titanium atoms, saturated with a TIP3P hydroxyl group (*OTX*, *HTX*)
O_{sat}	*ONX*	234	-0.990 to -0.492	oxygen atom protonated by hydrogen atom (*HBX*) of TIP3P to balance *TNX* saturation
O_t	*OTX*	234	-0.834	TIP3P oxygen to saturate *TNX*
H_t	*HTX*	234	0.417	TIP3P hydrogen to saturate *TNX*
H_s	*HBX*	234	0.417	TIP3P oxygen to protonate *ONX*
Ti_t	*HTI*	120	1.238 to 1.844	surface titanium, hydroxylated with TIP3P atoms (O_t, H_t)
O_t	*HTI*	120	-0.834	TIP3P water oxygen, hydroxylating O_t
H_t	*HTI*	120	0.417	TIP3P water hydrogen, hydroxylating O_t
Ti_t	*TI2*	254	1.150 to 1.944	surface titanium, dehydroxylated Ti_t/*HTI* version
O_s	*HTT*	66	-0.894 to -0.499	surface oxygen, protonated with TIP3P hydrogen (H_s)
H_s	*HTT*	66	0.417	TIP3P water hydrogen, protonating O_s/*HTT*
O_s	*OTT*	308	-1.146 to -0.597	surface oxygen, deprotonated O_s/*HTT* version

A.4 Water simulation setup

To evaluate the interaction of anions and cations in water with the TiO_2 surface without pollutants present, a simulation with an increased ion concentration has been computed. Here not only the surface neutralizing ions (54 Na^+) are present, but additional 0.10 mol/l sodium chloride ions (54 Na^+ and 54 Cl^-). In order to not let the neutralizing Na^+ block the surface, the simulation cell is divided into 4 areas A, B, C and D (Fig. A.4.1), that are defined by bias walls applied with PLUMED. To account for morphing cell volumes in the equilibration NpT ensemble, the walls are fixed to relative cell coordinates, spanning from -0.5 (-50 %) to 0.5 (50 %) in each direction.

The neutralizing Na^+ are distributed evenly in area A and D, away from the surface, ranging from 0.26 to 0.48 and from -0.26 to -0.48 in z-direction. Area B and C contain half of the additional ions each with z-coordinates ranging from 0.00 to 0.25 (B) and -0.25 to 0.00 (C). Throughout the first equilibration steps (cf. section A.5) a lighter bias with a force constant of 1500 kJ/(mol nm^2) is applied to all ions with the z-coordinate as collective variable (CV). For the annealing (step 7 in section A.5), the bias needed to withstand the increased temperature, so the force constant is changed to 5000 kJ/(mol nm^2). In the production run it was possible to lower it again to 1500 kJ/(mol nm^2).

A.5 Equilibration protocol

The equilibration is done in two parts: Since the simulation setup needs a careful heat up, the first three steps (energy minimization, NVT and NpT ensemble) contain a position restraint on the TiO_2 core atoms (Ti_b, Ti_{sat}, Ti_t, O_b, O_{sat}, O_s) and the pollutants with a force constant of 10,00 kJ/(mol nm^2) and 1000 kJ/(mol nm^2), respectively. Solely ions, water molecules and surface groups (O_t, H_t, H_s) are able to move. After the energy minimization, in the first NVT ensemble (step 2, Tab. A.5.1) the pollutants are kept at 100 K, while the other atoms are heated from 100 K to 300 K in a linear temperature ramp over the first 100 ps of the 200 ps trajectory. The final temperatures from step 2 are kept for the NpT equilibration in step 3.

In the second part, the position restraint on the pollutants is lifted. After a second energy minimization in step 4, the NVT starts with a 100 ps temperature ramp from 100 K to 300 K for the pollutants, while the other simulation parts are at 300 K from the beginning. In the NpT (step 6) all atoms are at a temperature of 300 K. As a last preparation a temperature annealing is done to reset all contacts that could have been established between the ions, water and pollutants with the surface (step 7). Here the whole system is heated from 300 K to 500 K in the first 300 ps, kept at 500 K for 400 ps and cooled down back to 300 K over another 300 ps. For 1 ns the temperature is kept constant at 300 K before the final production run is started. The production run (step 8) is calculated for 100 ns at a temperature of 300 K for the entire system and a position restraint is applied to the surface core atoms.

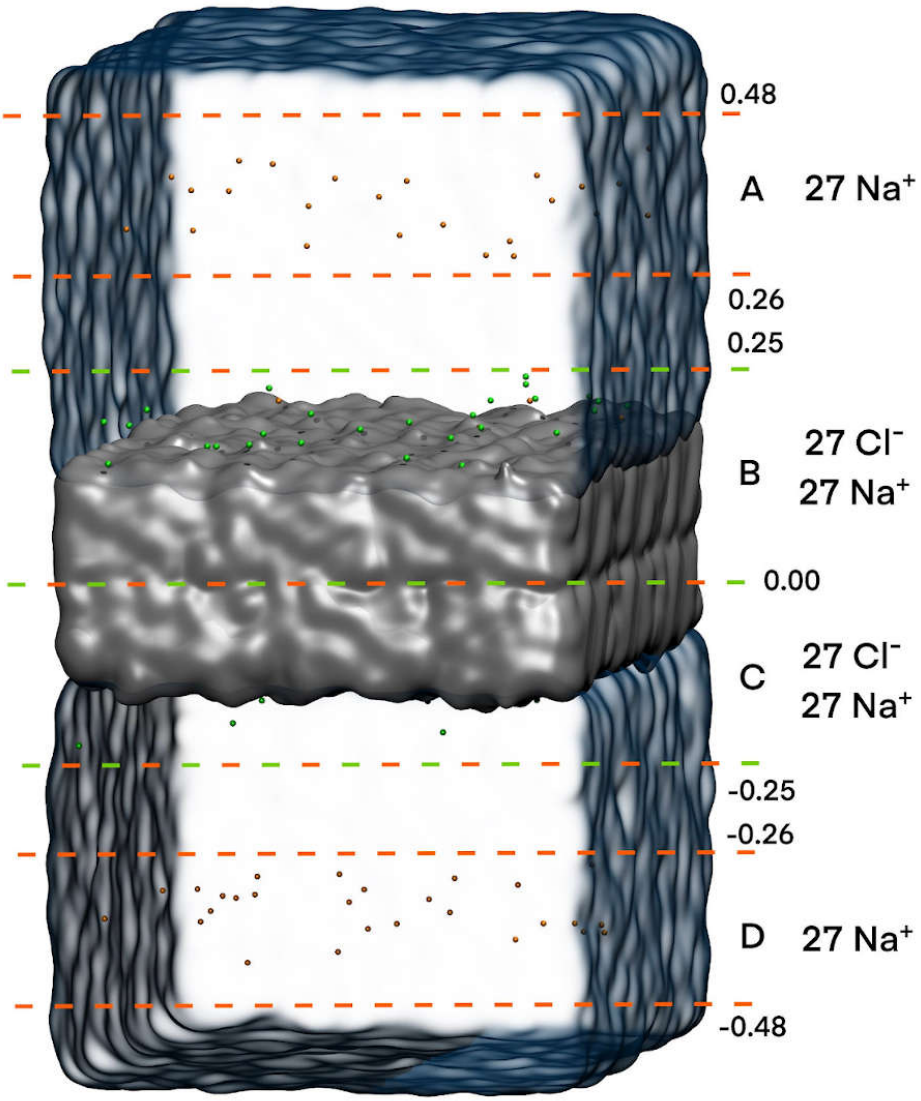

Fig. A.4.1 The simulation setup containing water (blue), the TiO_2 surface (silver) and an increased amount of Na^+ (orange) and Cl^- (green). The cell is divided into four areas (A, B, C and D) which are separated by bias walls (dashed lines, orange if they act on Na^+, green if they act on Cl^-). Areas A and D are containing 27 charge neutralizing Na^+ ions, while are B and C are holding 27 Na^+ and 27 Cl^- ions. The coordinates are relative, spanning from -0.5 to 0.5. Here the z coordinates for the bias walls are shown.

Table A.5.1 Steps in simulation equilibration for all pollutant systems with their respective ensemble (EM - energy minimization), their duration in ns, to which system parts a position restraint is applied and the pollutant, surface and water and ions temperatures in K. TiO_2 core atoms consist of Ti_b, Ti_{sat}, Ti_t, O_b, O_{sat} and O_s

step	ensemble	duration (ns)	position restraint	T_{POL} (K)	T_{TiO_2} (K)	$T_{H_2O\&ions}$ (K)
1	EM	-	POL & TiO_2 core atoms	-	-	-
2	NVT	0.2	POL & TiO_2 core atoms	100	100 - 300	100 - 300
3	NpT	0.1	POL & TiO_2 core atoms	100	300	300
4	EM	-	TiO_2 core atoms	-	-	-
5	NVT	0.3	TiO_2 core atoms	100 - 300	300	300
6	NpT	0.1	TiO_2 core atoms	300	300	300
7	NVT	2.0	TiO_2 core atoms	300 - 500	300 - 500	300 - 500
8	NVT	100.0	TiO_2 core atoms	300	300	300

A.6 Dipole moments

The dipole moments of pollutants with a different protonation state than zero are not reported as extensive as the dipole moments for their neutral form. Since we also calculated charges and dipole moments for the neutral forms in the same way as reported, we show the conformance of these neutral species here (Tab. A.6.1). The dipole moments are in fairly good agreement with literature values. Thus we conclude that the calculated CHELPG charges of the pollutant molecules are valid.

We find it important to note that we also calculated a geometry optimization and the CHELPG charges for TTR^0 in implicit water, and that it yielded a higher molecular dipole of 24.8 D, instead of 15.0 D in vacuum. The same calculation method was used to stabilize TTR^{-2} (plus a bias) and GGG^{-2}. It could be a hint that the partial charges could be more pronounced in these cases, which could lead to higher contact rates with the surface. But the dipole moment is a 1-dimensional and thus reduced characteristic of the molecule structure. It is highly dependent on torsional and dihedral angles and therefore changes greatly throughout the simulations, especially in tetracycline and glyphosate. We did not find a correlation between the dipole moment and the contact rate (cf. section 4.2), which strengthens the importance of 3-dimensional charge distribution over the molecule instead of the 1-dimensional dipole moment.

Table A.6.1 Dipole moments of neutral pollutant species, that are used in this study with non-neutral protonation states, as well as dipole moments from literature for comparison

POL	calculated dipole moment (D)	dipole moment from literature (D)
ASA^0	2.1	1.5 [10]
IBU^0	1.7	1.4 - 1.8 [11,12]
SLC^0	2.8	2.5 [13]
TTR^0	15.0	14.8 [14]
VLP^0	1.5	1.4 - 1.6 [15]

A.7 Adsorption modes over time

The adsorption modes of pollutants on TiO_2 over time can be found here (Fig. A.7.1, A.7.2, A.7.3 and A.7.4). All 25 pollutant molecules per simulation system are depicted for 100 ns of the production trajectory. Direct contacts, where distances between pollutant and surface atoms are smaller than 2.5 Å, are marked in blue, while indirect contacts (distances between 2.5 Å and 6.0 Å) are shown in yellow.

A.8 Relative distances of the functional groups of GGG^{-2}

The normalized densities over relative TiO_2 height (Fig. A.8.1) confirm the presumptions from the densities over cell height: The negative functional groups, especially carboxylate, are primarily found inside the first water oxygen layer ($OW_{[0]}$ density of reference simulation in background). If not in the first water oxygen layer, the functional groups peak on top of the second oxygen layer, which indicates the propensity of molecules that are blocked by the water layers.

A.9 Averaged contact numbers for GGG^{-2} and TTR^{-2}

The contact numbers for two individual GGG^{-2} and TTR^{-2} molecules, one solvated and one in contact with the surface, respectively, are calculated for 50 ns of the trajectory. The grey areas in Fig. 7 D to G show 2 ns windows that are distributed over the analysis to mark different states of the molecule: fully solvated, in contact with ions, in contact with other pollutant molecules of the same species etc.. The averaged numbers of these states can be seen in Tab. A.9.1 an A.9.2.

In Tab. A.9.3 the contact drifts for all GGG^{-2} and TTR^{-2} in the simulation cell, Na^+, water, the surface and the pollutant with itself are shown as averaged numbers of the first 1 ns (0 ns - 1 ns) and last 1 ns (99 ns - 100 ns) of the simulation time. The numbers of contacts are counted per molecule except for the surface contacts, these are counted per atom. The drifts are taken for the contact matrix (Fig. 9 E and F) in the main manuscript.

A.10 Hydrogen bridges between the pollutant and the surface

The water surrounding a pollutant that contacts the surface can build a network, which can be estimated through the average number of water bridges per frame (Fig. A.10.1). Here, 1st and 2nd order bridges between the pollutant and surface heavy atoms are considered. It is clearly observed that a huge network around TTR is building up regardless of the protonation state (99 and 243 water bridges per frame for TTR^{-1} and TTR^{-2}). All other molecules only form few water bridges in total, even GGG^{-2} with its multiple negative functional groups (3 per frame). Probably GGG^{-2}s attachment points for water bridges are occluded by ions or other GGG^{-2} molecules. These results suggest that the surrounding water network can stabilize the adsorbate, leading to long retention times, but it is not an exclusive criterion.

A.11 Solvent accessible surface areas (SASA)

The combined solvent accessible surface areas (SASA) of pollutants including the TiO_2 surface for neutral and singly negative protonation states are shown in Fig. A.11.1. The single value at -1 ns is the SASA of this combined group before equilibration. Most pollutants show only a small change from initial value to production run and a stable behavior. Only the clustering pollutants (CAF^0, CBZ^0 and TTR^{-1}) show a decrease in their SASA, which is due to their aggregation and, in the case of TTR^{-1}, also to their adsorption to the surface. The low initial SASA of IBU^{-1} is a result of the initial system geometry: The ibuprofen molecules are less than their van der Waals radius plus the SASA radius (two times 1.4 Å) away from each other. Thus, they are forming SASA cluster with a lowered area until they are equilibrated and free to move.

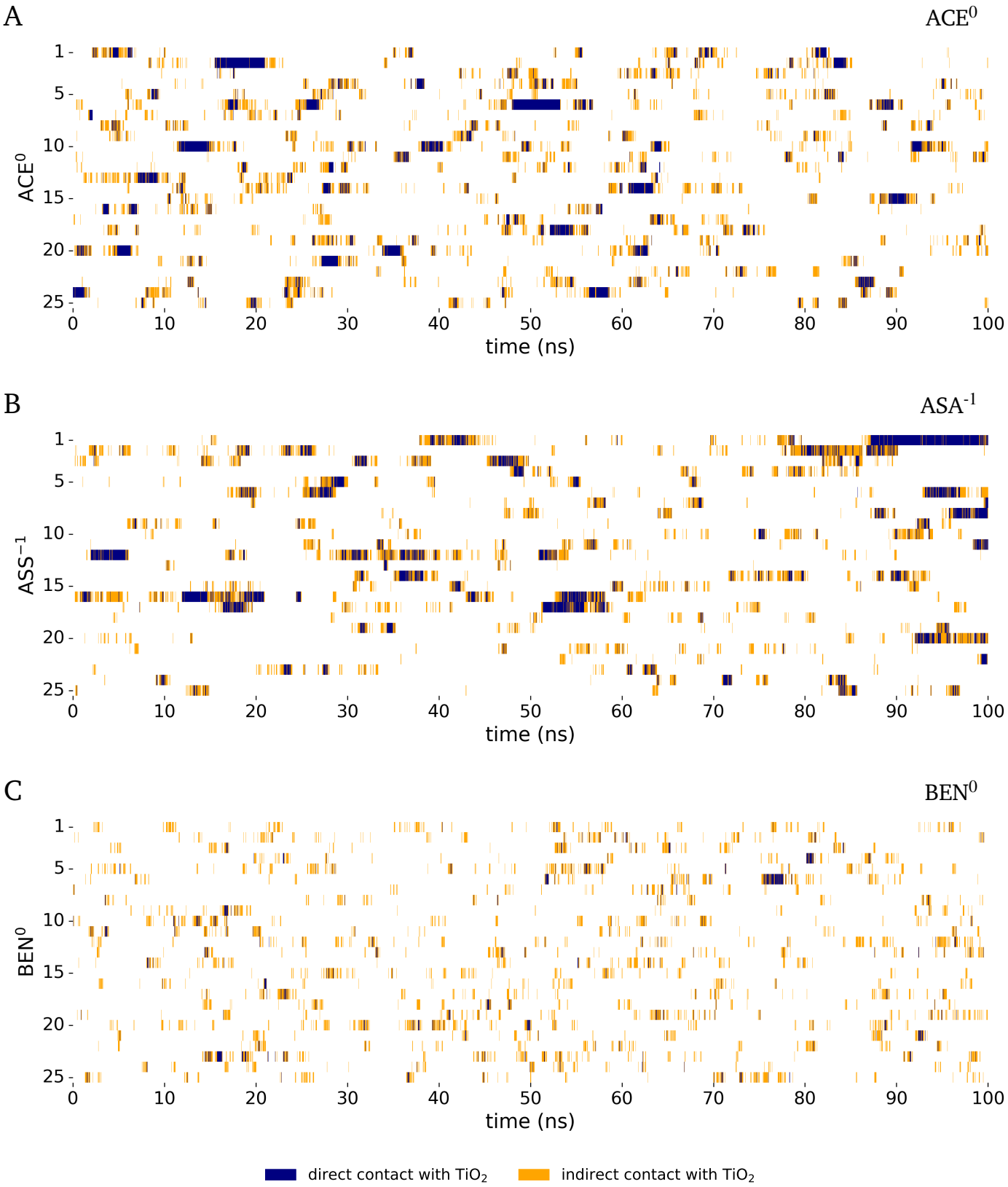

Fig. A.7.1 Contacts of pollutant molecules with TiO_2 over simulation time. Here the contact patterns for ACE^0 (A), ASA^{-1} (B) and BEN^0 (C) are shown for all 25 pollutant molecules over 100 ns. Blue regions mark direct contact between the pollutant and the surface, meaning a distance less than 2.5 Å, while orange marks indirect contacts, thus distances between 2.5 Å and 6.0 Å.

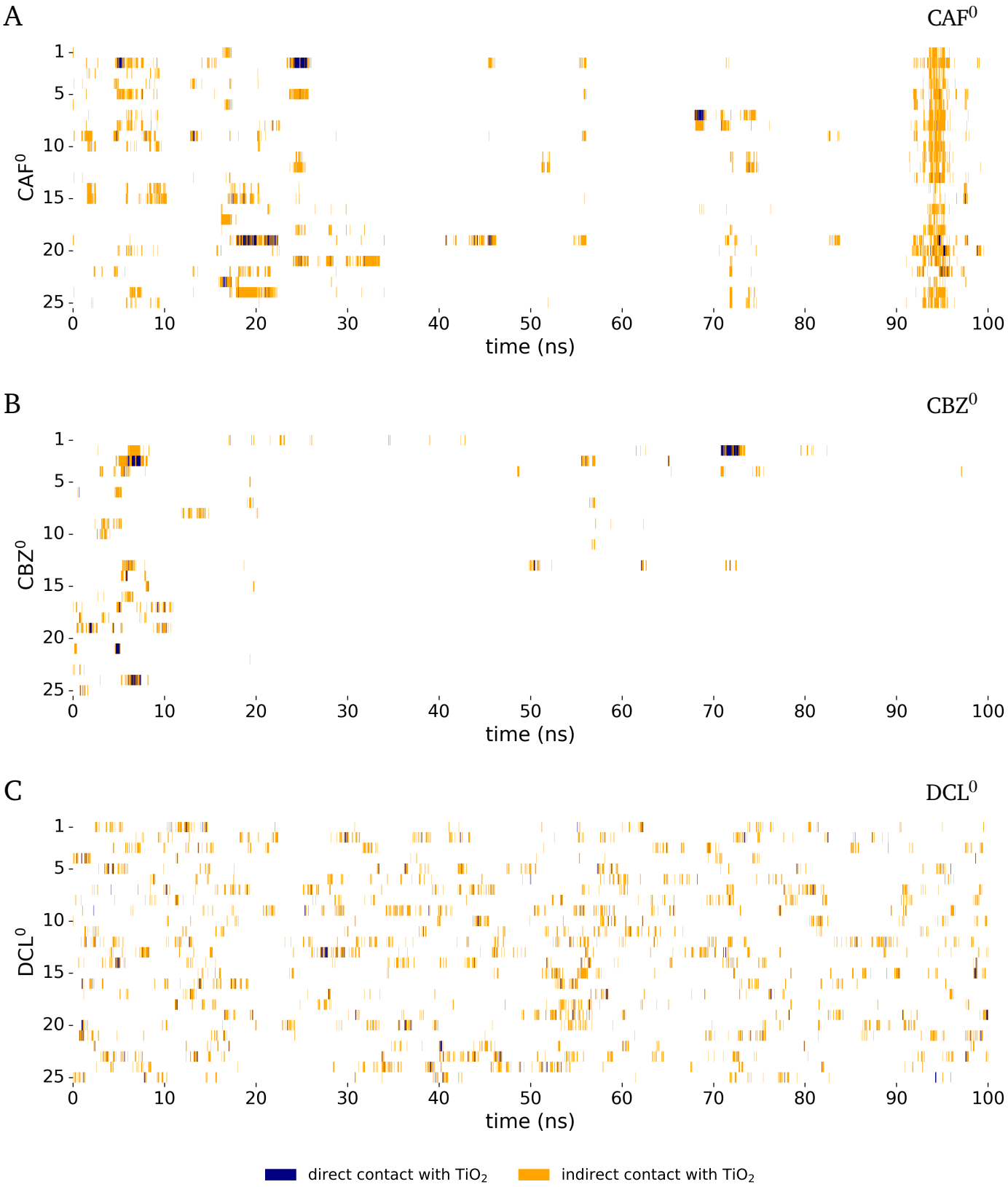

Fig. A.7.2 Contacts of pollutant molecules with TiO_2 over simulation time. Here the contact patterns for CAF^0 (A), CBZ^0 (B) and DCL^0 (C) are shown for all 25 pollutant molecules over 100 ns. Blue regions mark direct contact between the pollutant and the surface, meaning a distance less than 2.5 Å, while orange marks indirect contacts, thus distances between 2.5 Å and 6.0 Å.

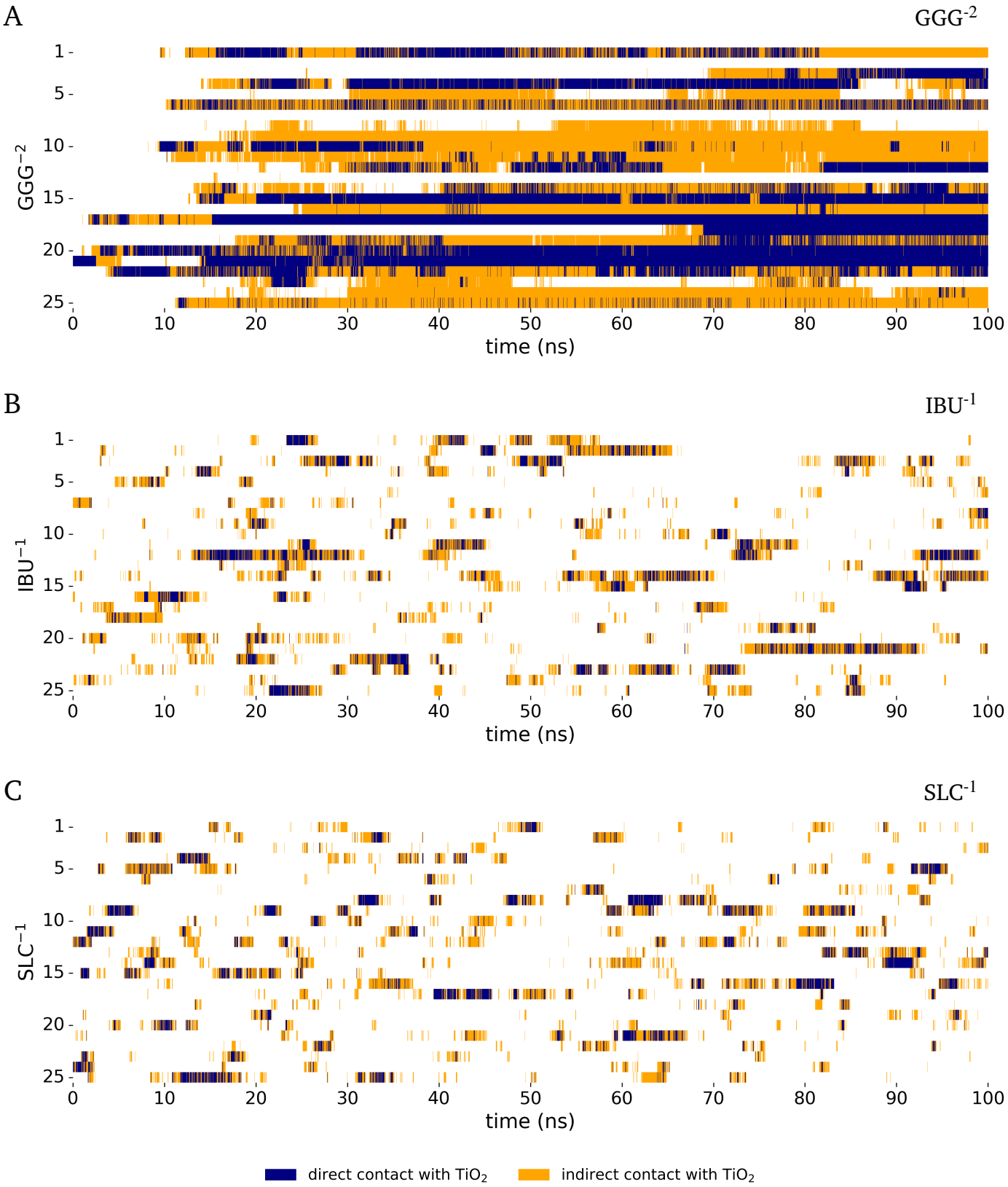

Fig. A.7.3 Contacts of pollutant molecules with TiO_2 over simulation time. Here the contact patterns for GGG^{-2} (A), IBU^{-1} (B) and SLC^{-1} (C) are shown for all 25 pollutant molecules over 100 ns. Blue regions mark direct contact between the pollutant and the surface, meaning a distance less than 2.5 Å, while orange marks indirect contacts, thus distances between 2.5 Å and 6.0 Å.

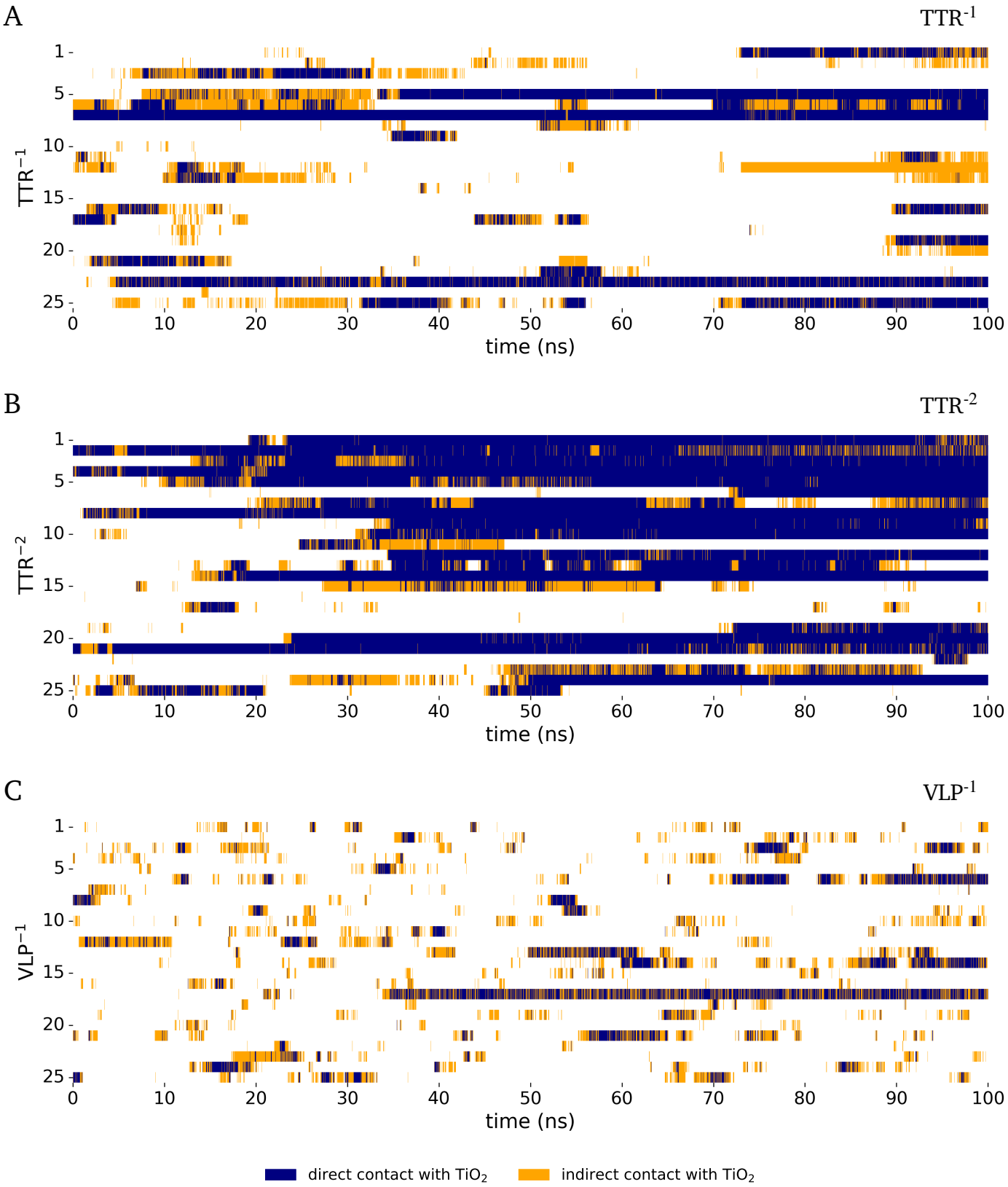

Fig. A.7.4 Contacts of pollutant molecules with TiO_2 over simulation time. Here the contact patterns for TTR^{-1} (A), TTR^{-2} (B) and VLP^{-1} (C) are shown for all 25 pollutant molecules over 100 ns. Blue regions mark direct contact between the pollutant and the surface, meaning a distance less than 2.5 Å, while orange marks indirect contacts, thus distances between 2.5 Å and 6.0 Å.

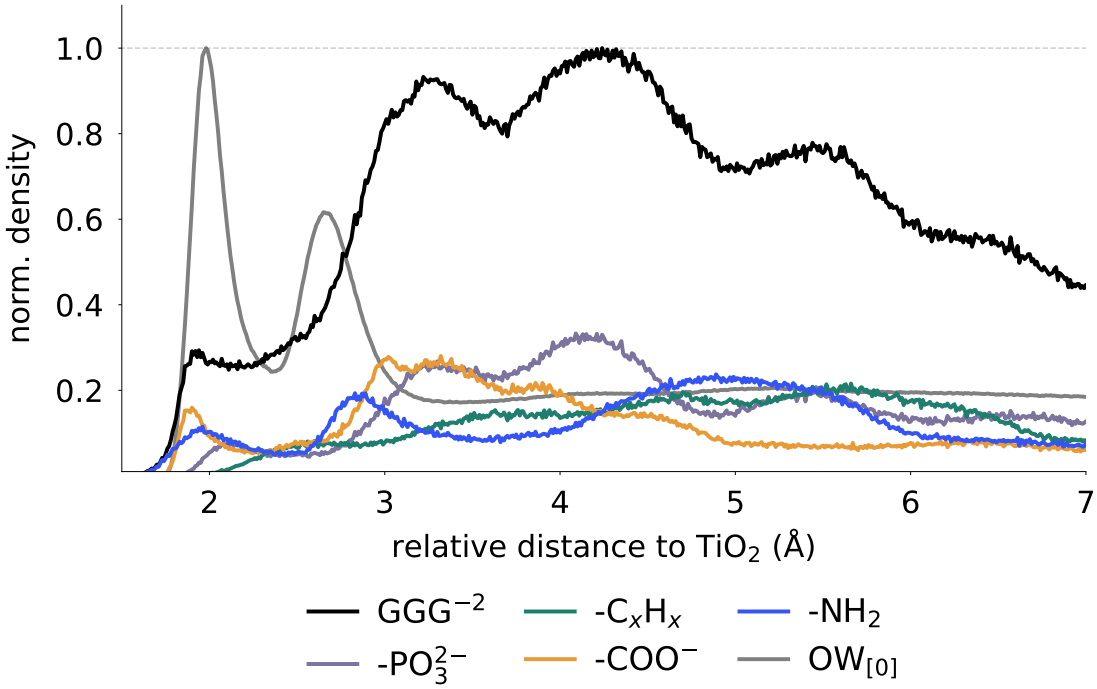

Fig. A.8.1 Relative distance plot of GGG^{-2}, underlaid with the relative distance of water oxygen from the reference simulation (cf. Fig. 2 B). GGG^{-2} possesses a carboxylate group pointing to the surface, that is located inside the first water oxygen peak or above the second hydration shell, reaching closest to the TiO_2 surface.

Table A.9.1 Averaged contact numbers of two individual GGG^{-2} molecules with water, ions and other GGG^{-2} per molecule, as well as TiO_2 per atom. Various 2 ns windows of the trajectory are chosen to depict different circumstances of contacts for the molecules

		averaged number of contacts			
identity	time (ns)	H_2O	Na^+	TiO_2	GGG^{-2}
GGG^{-2} in water	3.5 – 5.5	18.97	0	0	0
GGG^{-2} in water	22 – 24	17.23	0.99	0	0
GGG^{-2} in water	34 – 36	19.04	0	0	0
GGG^{-2} at surface	8 – 10	13.31	1.94	6.32	0
GGG^{-2} at surface	17 – 19	14.31	1.98	4.1	0
GGG^{-2} at surface	27 – 29	15.59	1.16	4.26	0

Table A.9.2 Averaged contact numbers of two individual TTR^{-2} molecules with water, ions and other TTR^{-2} per molecule, as well as TiO_2 per atom. Various 2 ns windows of the trajectory are chosen to depict different circumstances of contacts for the molecules

		averaged number of contacts			
identity	time (ns)	H_2O	Na^+	TiO_2	TTR^{-2}
TTR^{-2} in water	14.5 – 16.5	19.30	2.53	0.00	0.52
TTR^{-2} in water	21 – 23	22.30	0.99	0.00	0.00
TTR^{-2} in water	25 – 27	24.45	0.00	0.00	0.00
TTR^{-2} at surface	1 – 3	23.09	0.97	1.70	0.00
TTR^{-2} at surface	13 – 15	23.53	0.00	3.86	0.00
TTR^{-2} at surface	43.5 – 45.5	25.07	0.00	2.30	0.00

Table A.9.3 Averaged contact numbers of all TTR^{-2} and GGG^{-2} molecules in the cell with water, ions and other pollutants per molecule, as well as TiO_2 per atom. The initial number is derived from the average of the first (0 ns - 1 ns), the final number from the last nanosecond of the simulation (99 ns - 100 ns)

		averaged number of contacts						
pollutant	time (ns)	POL - H_2O	POL - TiO_2	POL - Na^+	POL - POL	Na^+ - H_2O	Na^+ - TiO_2	TiO_2 - H_2O
GGG^{-2}	0 - 1	341.84	2.62	37.34	19.85	96.86	39.59	1653.43
GGG^{-2}	99 - 100	280.18	20.86	46.86	40.92	89.68	61.90	1619.80
TTR^{-2}	0 - 1	531.25	5.54	17.22	8.43	98.45	43.72	1668.47
TTR^{-2}	99 - 100	562.64	40.99	16.80	4.00	97.16	65.96	1624.01

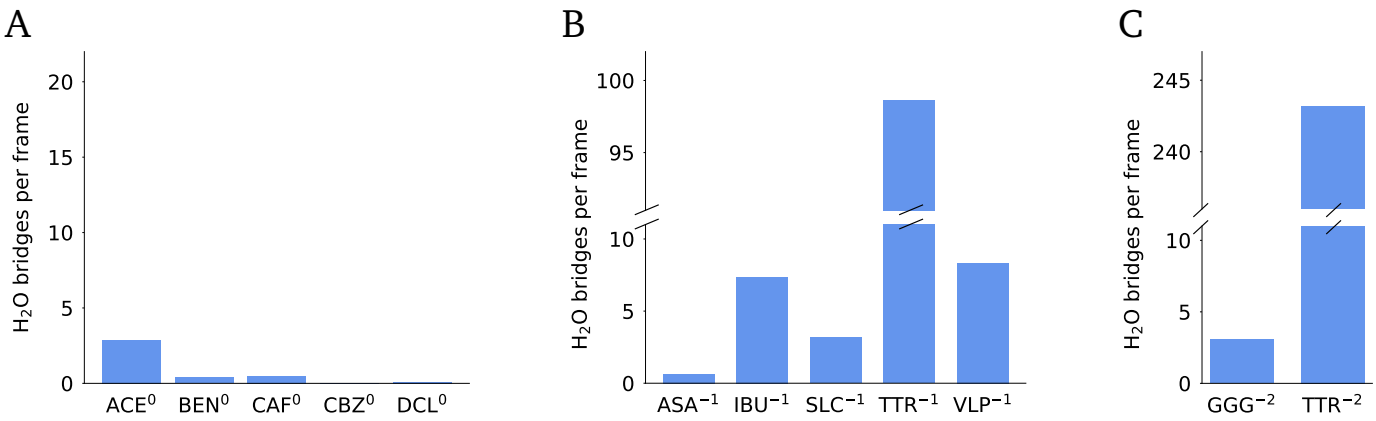

Fig. A.10.1 Averaged number of 1st and 2nd order H_2O bridges per frame for all pollutants. It is striking that TTR seems to form big water networks, independent of its protonation state.

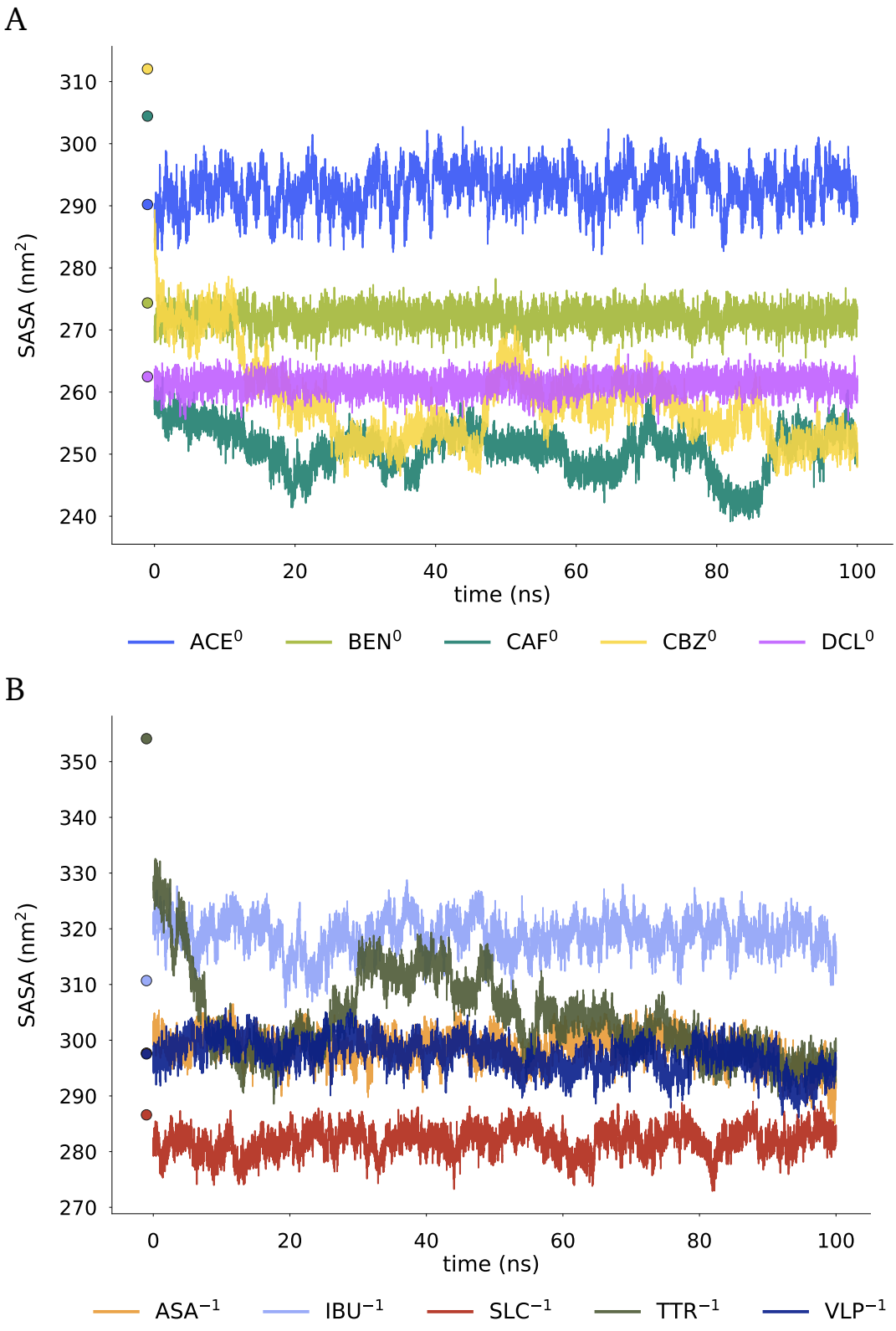

Fig. A.11.1 Solvent accessible surface areas (SASA) of the TiO_2 surface and pollutants combined before equilibration (-1 ns, single data point) and over the production run. A) shows the pollutants with neutral and B) with single negative protonation state.

References

1 M. M. Peixoto, G. F. Bauerfeldt, M. H. Herbst, M. S. Pereira and C. O. da Silva, *J. Phys. Chem. A*, 2015, **119**, 5241–5249.

2 B. Liu, L. Dong, Q. Yu, X. Li, F. Wu, Z. Tan and S. Luo, *J. Phys. Chem. B*, 2016, **120**, 2132–2137.

3 M. Sadatsharifi, D. W. Ingersoll and M. Purgel, *Environ. Sci.: Processes Impacts*, 2021, **23**, 1018–1028.

4 P. Sprankle, W. F. Meggitt and D. Penner, *Weed Sci.*, 1975, **23**, 229–234.

5 M. Muneer and C. Boxall, *Int. J. Photoenergy*, 2008, **2008**, 197346.

6 E. Vidal, A. Negro, A. Cassano and C. Zalazar, *Photochem. Photobiol. Sci.*, 2015, **14**, 366–377.

7 W. Zuo, N. Li, B. Chen, C. Zhang, Q. Li and M. Yan, *Sci. Total Environ.*, 2020, **726**, 138432.

8 A. Amat, S. Fantacci, F. De Angelis, B. Carlotti and F. Elisei, *Theor. Chem. Acc.*, 2012, **131**, 1218.

9 L. Derr, N. Hildebrand, S. Köppen, S. Kunze, L. Treccani, R. Dringen, K. Rezwan and L. Colombi Ciacchi, *Biointerphases*, 2016, **11**, 011007.

10 Y. Lee, D.-G. Kwon, G. Kim and Y.-K. Kwon, *Phys. Chem. Chem. Phys.*, 2017, **19**, 8076–8081.

11 M. L. Vueba, M. E. Pina and L. A. E. Batista de Carvalho, *J. Pharm. Sci. (Philadelphia, PA, U. S.)*, 2008, **97**, 845–859.

12 A. R. Brás, J. P. Noronha, A. M. M. Antunes, M. M. Cardoso, A. Schönhals, F. Affouard, M. Dionísio and N. T. Correia, *J. Phys. Chem. B*, 2008, **112**, 11087–11099.

13 A. L. Sobolewski and W. Domcke, *Chem. Phys.*, 1998, **232**, 257–265.

14 B. Mecheri, F. Gambinossi, M. Nocentini, M. Puggelli and G. Caminati, *Biophys. Chem.*, 2004, **111**, 15–26.

15 H. M. Badawi, W. Förner and S. A. Ali, *J. Mol. Struct.*, 2014, **1075**, 494–503.